GISC 7365: Advanced Remote Sensing Final Project Report

Analyzing forest fires using Active fire detection algorithm from Landsat 8 OLI/TRS Data – A case study of Thomas fire occurred in Santa Barbara and Ventura Counties, California.

Submitted by: Rohit Venkat Gandhi Mendadhala

Instructor: Dr. Fang Qiu

May 1st, 2018

Contents

1. Introduction and Background:

One of the most common hazard in forests in forest fire. These are almost as old as forests themselves. Forest Fires may be sometimes good for ecological processes. However, their negative effects surpass the benefits and creates a big threat to environment, human life and economy. Forest fires are caused either naturally or by human interaction. Natural fires are usually started with a great lightening effect leading to a small percentage of combustion of dry fuel like sawdust and leaves. Unlike natural fires, human caused fires are originated due to smoking, recreation and other miscellaneous activities. Even though human caused fires constitute greater percentage of ignited forest fires, majority of the burnt area is caused because of the natural fire. This is because of the fact that human caused fires are immediately detected in their early duration thereby leading them to be contained easily. On the flip side natural fires can burn and destroy landcover for hours before any detection is made by fire fighters.

In the recent times, US has lost a considerable amount of forests because of conversion of the land cover into agricultural lands and many other forms. As per 2017 annual wild fire assessment report by National Interagency Coordination Center, there was approximately more than 40,000 acres that was burnt due to wildfires. The largest fire being the Thomas fire, brought an estimate loss of $123,836,000 approximately. This made me to understand, detect and analyze the occurrences of forest fires. It also urged me to make pre-fire, post fire and on fire assessment using Satellite Image Analysis by taking Thomas fire as a case study which has been the largest wild fire in the history of California.

2. How can Remote Sensing and GIS aid in analyzing forest fires?

2.1 Pre-fire Planning:

- Helps in estimating vegetation dryness there by allowing us to make maps and monitor this.
- Helps in fire tower visibility analysis etc.
- Aids in Fuel Type Mapping (Eg. Arc Fuel)

2.2 During Fire:

- Fire Assist operations can be performed for suppressing the fires with the help of fire fighters.

2.3 Post Fire- Impact Assessment:

- For performing burnt area mapping and change mapping using Normalized Burned Ratio technique.
- Also helps in operational burned area mapping at a National Level.
- Burn Severity Mapping or Differenced Normalized Burn Ratio Mapping.
- Short and long-term damage assessment can be made.

3. Objectives:

- Analyzing Thomas Fire Occurrences.
- Applying decision rules based on literature for identifying fire pixels.
- Automating Batch Composite Imagery Generation for Image Analysis.
- Generating burn severity map post Thomas fire using NBR.
- Comparison of obtained fire pixels with Modis Data.

4. Thomas Fire and its overview:

Thomas fire is a massive wild fire which deeply affected Santa Barbara and Ventura Counties in Southern California in 2017. It has burnt approximately 282,000 acres becoming the largest wild fire in the modern history of California. Starting December 4th 2017, Thomas Fire was fully contained on January 12, 2018. Whether Thomas Fire is caused because of a human interaction or a natural factor is still under investigation. It is one of the multiple wildfires which ignited California in 2017.

The other fires caused are Rye Fire, Creek Fire. The fatalities caused by Thomas fire include 1 fire fighter, 1 civilian and 20 civilian indirectly got affected due to mud/debris flow in 2018. The non-fatalities include 2 fire fighters.

Terra Satellite Photo of smoke plumes

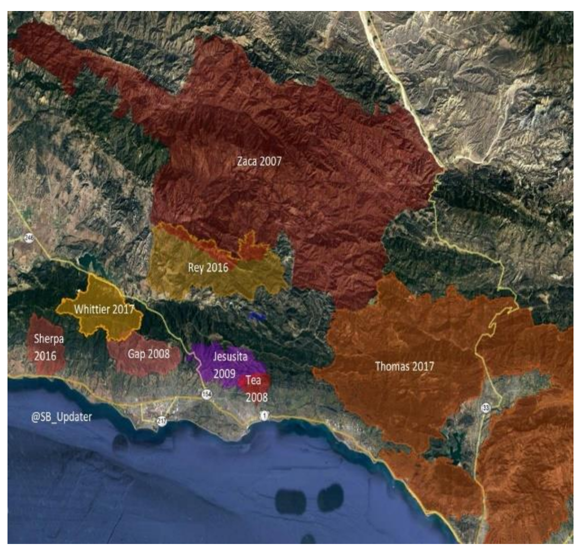

Thomas Fire Burn Scars seen from LandSAT 8

5. Study Area and Data Acquisition:

The study area chosen for analyzing Thomas fire is a combined area of Santa Barbara and Ventura Counties. Both the county shapefiles have been merged as a single shapefile and was taken as a reference for the overlaying satellite imagery acquired from USGS.

To analyze Thomas fire, we have taken Landsat 8 (OLI/TRS) Level 2 data was acquired. Foot prints were selected carefully so that maximum area is covered in the tile that are selected. The satellite imagery was acquired for the dates 23rd November, 9th December, 25th December, 10th January and 26th January. The dates were chosen based on the availability of the product data and also on the occurrence of Thomas Fire. As per the world-wide reference system the path and row of the data acquired was 42 and 36. The projection system being Universal Transverse Mercator (UTM) with Zone 11 and also the datum is WGS 1984.

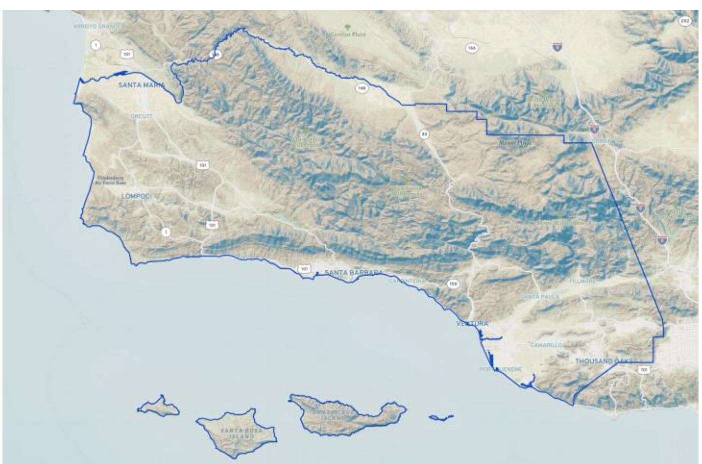

Hill Shaded representation of Santa Barbara and Ventura Counties, CA from MapBox

Table 1. Display and comparison of the bands and wavelengths of each Landsat sensor. Instrument-specific relative spectral response functions can be viewed and compared using the U.S. Geological Survey Spectral Viewer tool: https://landsat.usgs.gov/spectral-characteristics-viewer.

[OLI, Operational Land Imager; TIRS, Thermal Infrared Sensor; ETM+, Enhanced Thematic Mapper Plus; TM, Thematic Mapper; MSS, Multispectral Scanner; --, not applicable]

Band designations	Landsat band wavelength comparisons All bands 30-meter resolution unless noted									
	L8 OLI/TIRS		L7 ETM+		L4-5 TM		L4-5 MSS*		L1-3 MSS*	
Coastal/Aerosol	Band 1	0.43–0.45	--	--	--	--	--	--	--	--
Blue	Band 2	0.45–0.51	Band 1	0.45–0.52	Band 1	0.45–0.52	--	--	--	--
Green	Band 3	0.53–0.59	Band 2	0.52–0.60	Band 2	0.52–0.60	Band 1	0.5–0.6 *	Band 4	0.5–0.6 *
Panchromatic	Band 8**	0.50–0.68	Band 8 **	0.52–0.90	--	--	--	--	--	--
Red	Band 4	0.64–0.67	Band 3	0.63–0.69	Band 3	0.63–0.69	Band 2	0.6–0.7 *	Band 5	0.6–0.7 *
Near-Infrared	Band 5	0.85–0.88	Band 4	0.77–0.90	Band 4	0.76–0.90	Band 3	0.7–0.8 *	Band 6	0.7–0.8 *
Near-Infrared	--	--	--	--	--	--	Band 4	0.8–1.1 *	Band 7	0.8–1.1*
Cirrus	Band 9	1.36–1.38	--	--	--	--				
Shortwave Infrared-1	Band 6	1.57–1.65	Band 5	1.55–1.75	Band 5	1.55–1.75				
Shortwave Infrared-2	Band 7	2.11–2.29	Band 7	2.09–2.35	Band 7	2.08–2.35				
Thermal	Band 10 T1	10.60–11.19	Band 6 T2	10.40–12.50	Band 6 T2	10.40–12.50				
Thermal	Band 11 T1	11.50–12.51	--	--	--	--				

* Acquired at 79 meters, resampled to 60 meters
** 15-meter (panchromatic)
T1 = Thermal (acquired at 100 meters, resampled to 30 meters)
T2 = Thermal (acquired at 120 meters, resampled to 30 meters)

(Source: USGS, Landsat 8)

23rd Nov 2017

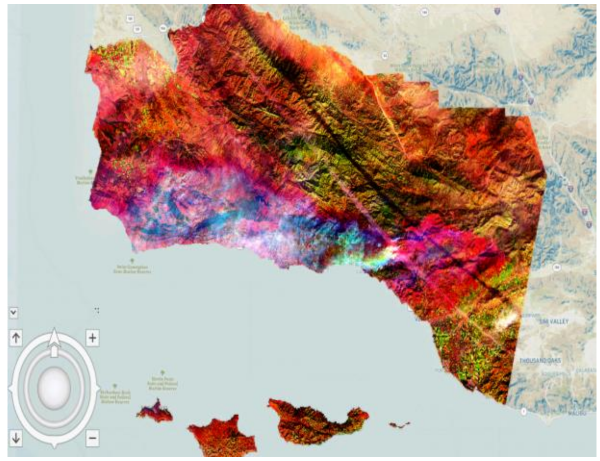

9th Dec 2017

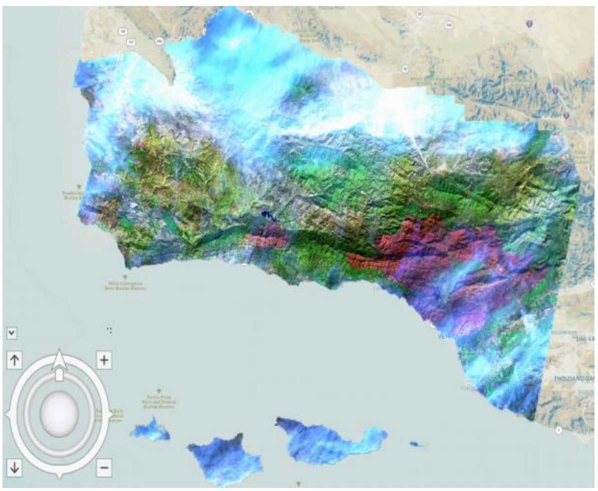

25th Dec, 2017

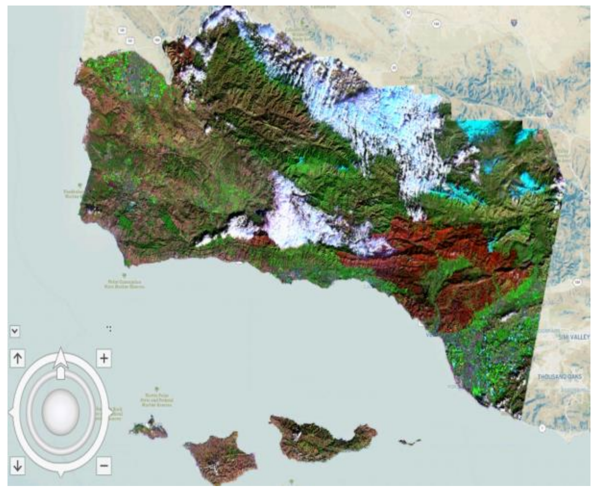

10th Jan, 2018

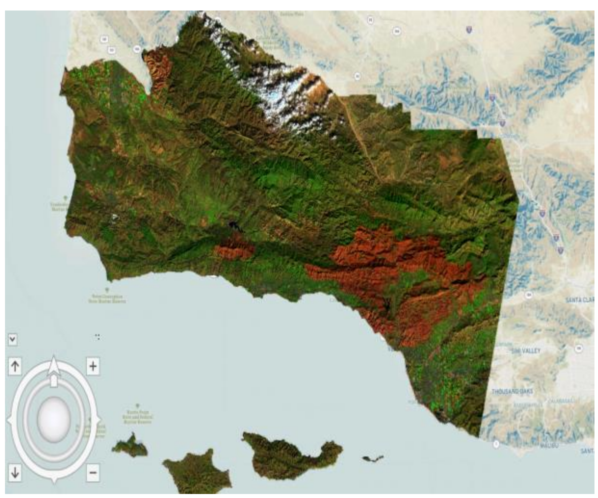

26th Jan, 2018

Landsat Imagery of Santa Barbara and Ventura counties before, after and during Thomas Fire. Bands 7,5,2 Combinations for detecting burn scars.

6. Batch Composite Raster Creation using ArcPy package from Pycharm IDE:

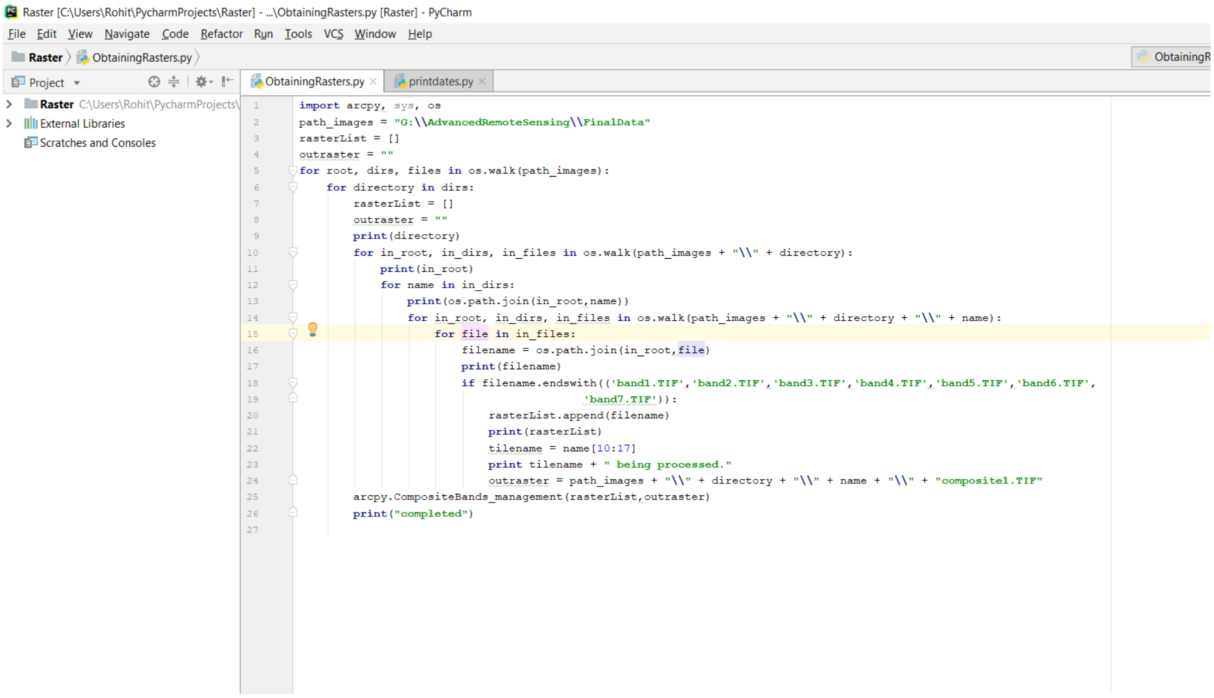

7. Methodology:

7.1 Conversion to TOA reflectance:

To have an effective result, all satellite images are converted to Top of Atmosphere reflectance (TOA) before processing. The importance of converting the image from Digital Numbers DNs to TOA reflectance is that the resulting TOA reflectance image represents the solar radiation incident on the instrument in a standard and unit less quantity, independent of the position of the sun with respect to the earth. This is advantageous when the satellite image is compared to other TOA reflectance images captured at a different date. The difference observed will mainly be due to changes on the surface of the earth and not due to differences in solar angles. For Landsat 8 OLI images following equations are used to convert image DNs to TOA reflectance

$$\rho'_\lambda = M_\rho Q_{cal} + A_\rho \qquad \text{--1}$$

$$\rho_\lambda = \frac{\rho_\lambda'}{\mathrm{Sin}(\theta_{SE})} \qquad \text{--2}$$

ρ_λ is TOA reflectance without correction for solar angle, is TOA planetary reflectance,

SE is the solar elevation angle,

$M\rho$ is band-specific multiplicative rescaling factor

$A\rho$is the band specific additive rescaling factor and

Qcal is the quantized and calibrated standard product pixel values meaning the image. All the above mentioned parameters can be obtained from MTL file of the downloaded data product.

7.2 Active Fire Algorithm:

Landsat 8 active fire detection algorithm is driven by fire sensitive SWIR channel (band) 7 data, exploiting the emissive component of fires in that spectral window. During day time emissive component is mixed with the background, which is dominated by the reflected solar component.

The algorithm uses input data from all seven OLI channels. The first test is designed to identify potentially unambiguous active fire pixels. It builds on the ETM+ active fire algorithm (Schroeder et al., 2008) while accommodating small differences in OLI spectral channels, and is based on the following condition:

Test 1 $R_{75} > 2.5 \ \& \ R_7 - R_5 > 0.3 \ \& \ R_7 > 0.5$

Highly energetic and extensive fires can lead to DN saturation on channel 7 thereby characterizing another condition of potentially unambiguous active fire pixel

Test 2: $R_6 > 0.8 \ \& \ R_1 < 0.2 \ \& \ (R_5 > 0.4 \mid R_4 < 0.1)$

Complementing the identification of unambiguous pixels, the thresholds in test 1 are relaxed and other fire pixels are selected further analysis based on the following criteria

Test 3A: $R_{75} > 1.8 \ \& \ R_7 - R_5 > 0.17$

All pixels satisfying the test 3A should also satisfy test 3B to be classified as potentially affected fire pixels.

Test 3B:

$R_{75} > mean(R_{75}) + max(\ sd(R_{75}), 0.8)$

$R_7 > mean(R_7) + max(\ 3.sd(R_7), 0.08)$

$R_{76} > 1.6$

R_i – Reflectance of band I, R_{ij} - Reflectance ratio of band i to j, Sd – Standard Deviation.

7.3 Why SWIR band is considered over TIR band for fire detection?

Thermal sensors usually capture imagery of warm objects against a cool background and they do not provide a good resolution (100m in Landsat 8) imagery. On the other hand, SWIR sensors have high resolution (30 m in Landsat 8) can identify what actually the object is. They can also pin point sites of active burning, detect hot spots and estimate where the fire is burning the hottest. This helps in directing the rescue team most efficiently.

7.4 Normalized Burn Ratio and Generation of Burn Severity Map:

The normalized burn ration (NBR) was specifically designed to highlight the burnt areas and also estimating fire severity. It is similar to NDVI, except it uses the near infrared (NIR) and shortwave-infrared (SWIR) wavelengths. The use of NDVI is based on the notion that healthy vegetation has high spectral reflectance in the Near-Infrared (NIR) and low spectral reflectance in the visible. The downfall of using NDVI for mapping burned areas is that it confuses the spectral signature of burned areas with that of water and shadows. Hence NBR is formulated as:

$$NBR = \frac{NIR-SWIR}{NIR+SWIR}$$

7.4.1 Burn Severity:

Imagery collected before a fire will have a very high infrared values and low mid infrared values, which is exactly inverse for the imagery collected after a fire. Normalized Burn Difference is given by

$$dNBR \text{ or } \Delta NBR = PrefireNBR - PostfireNBR$$

Higher the dNBR, higher the damage. In case if we have areas with a negative dNBR values, then it means there is an increased vegetation productivity after a fire. In general, the dNBR values can vary from scene to scene and best interpretation can be done only with a ground truth data collection. Typically, NBR and dNBR are generally calculated immediately after a wild fire occurs in order to know the percentage of the burnt area and also about the fire severity. This typically help us in estimating the likely future downstream impacts caused due to flooding, landslides or soil erosion.

dNBR	
< -0.25	High post-fire regrowth
-0.25 to -0.1	Low post-fire regrowth
-0.1 to 0.1	Unburned
0.1 to 0.27	Low-severity burn
0.27 to 0.44	Moderate-low severity burn
0.44 to 0.66	Moderate-high severity burn
>0.66	High-severity burn

8. Results:

Active Fire Pixel detection from Landsat 8 data - 9th Dec, 2017

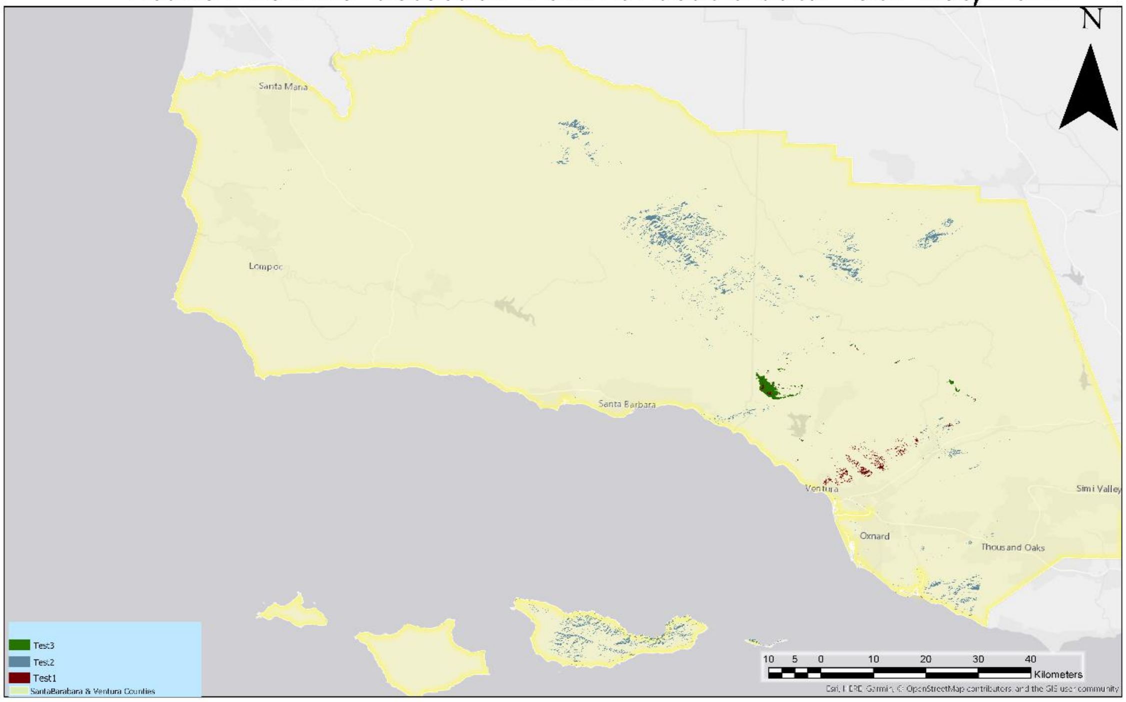

Fire Pixel Extractions

Active Fire Pixel detection from Landsat 8 data - 25th Dec, 2017

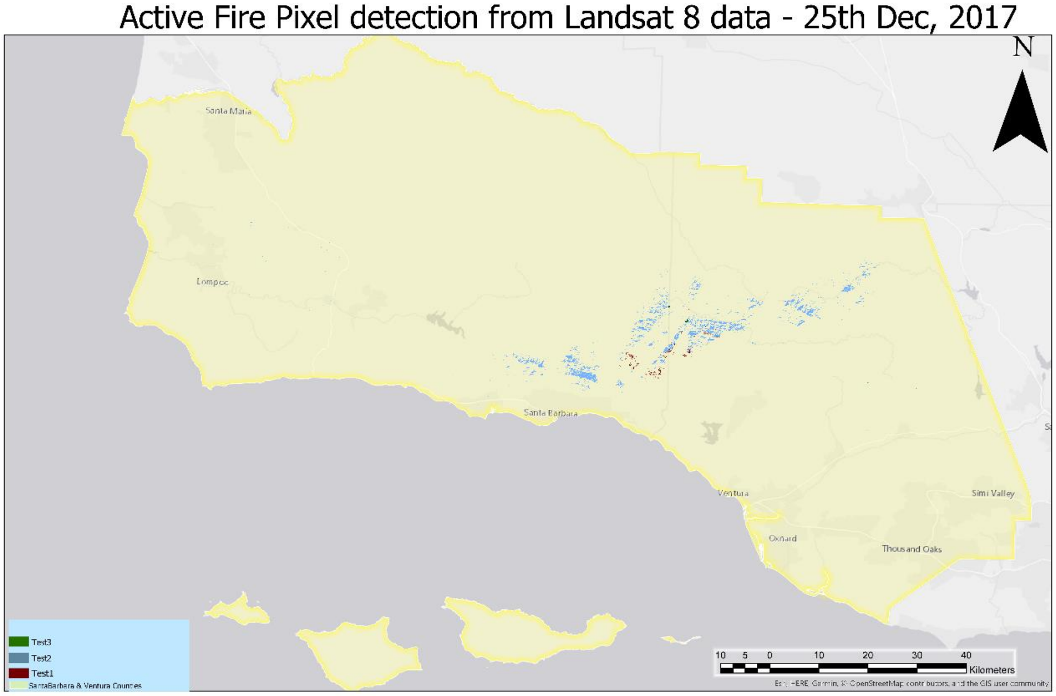

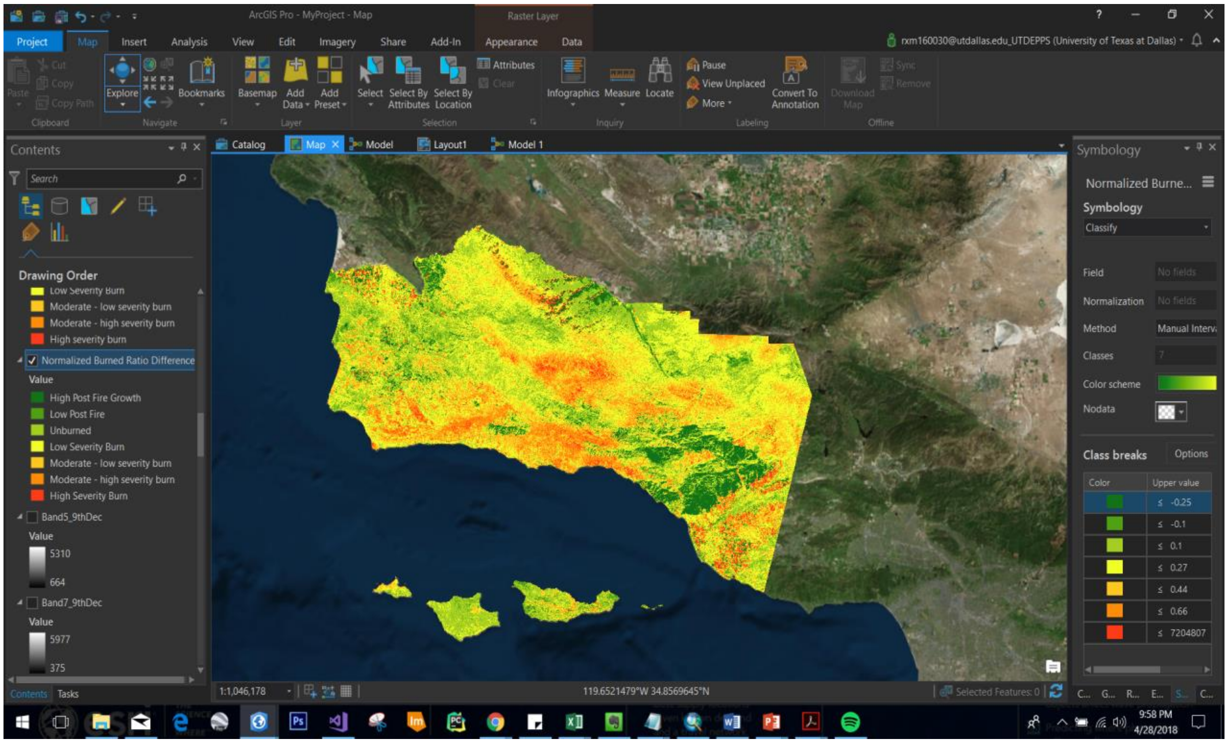

Burn Severity Mapping (ArcGIS Pro Data View and Layout View)

Burn Severity Difference (Pre and Post Thomas Fire)

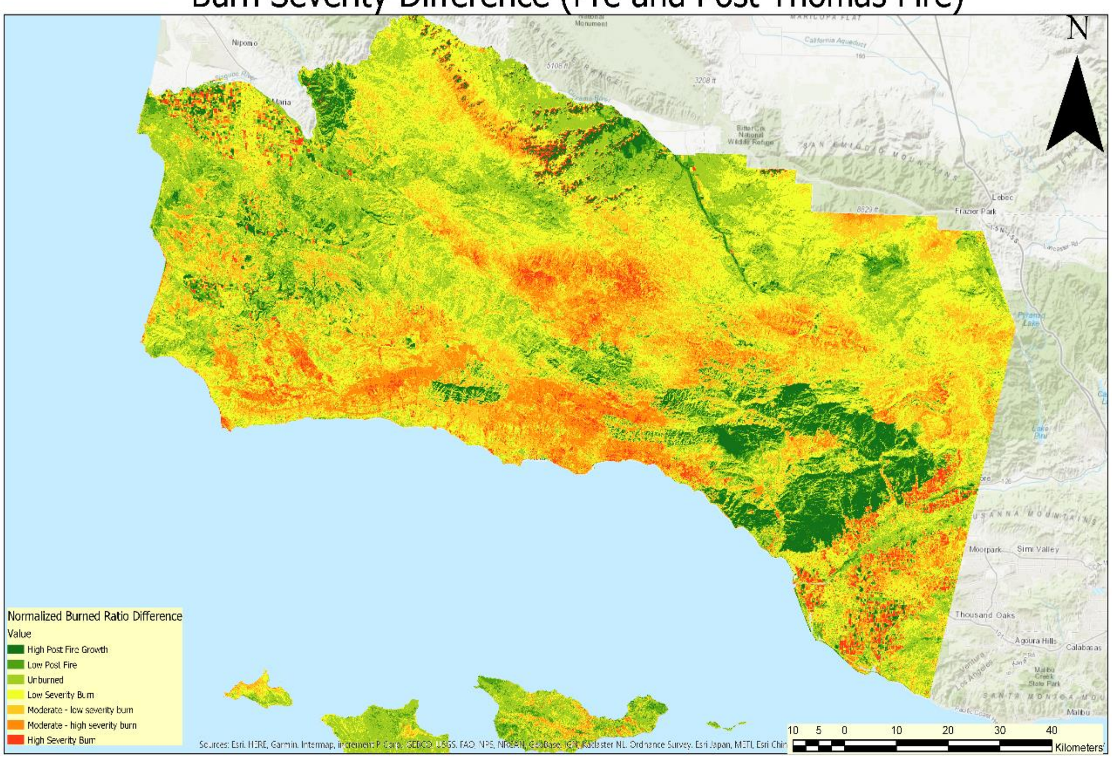

9. MODIS Imagery during Thomas Fire.

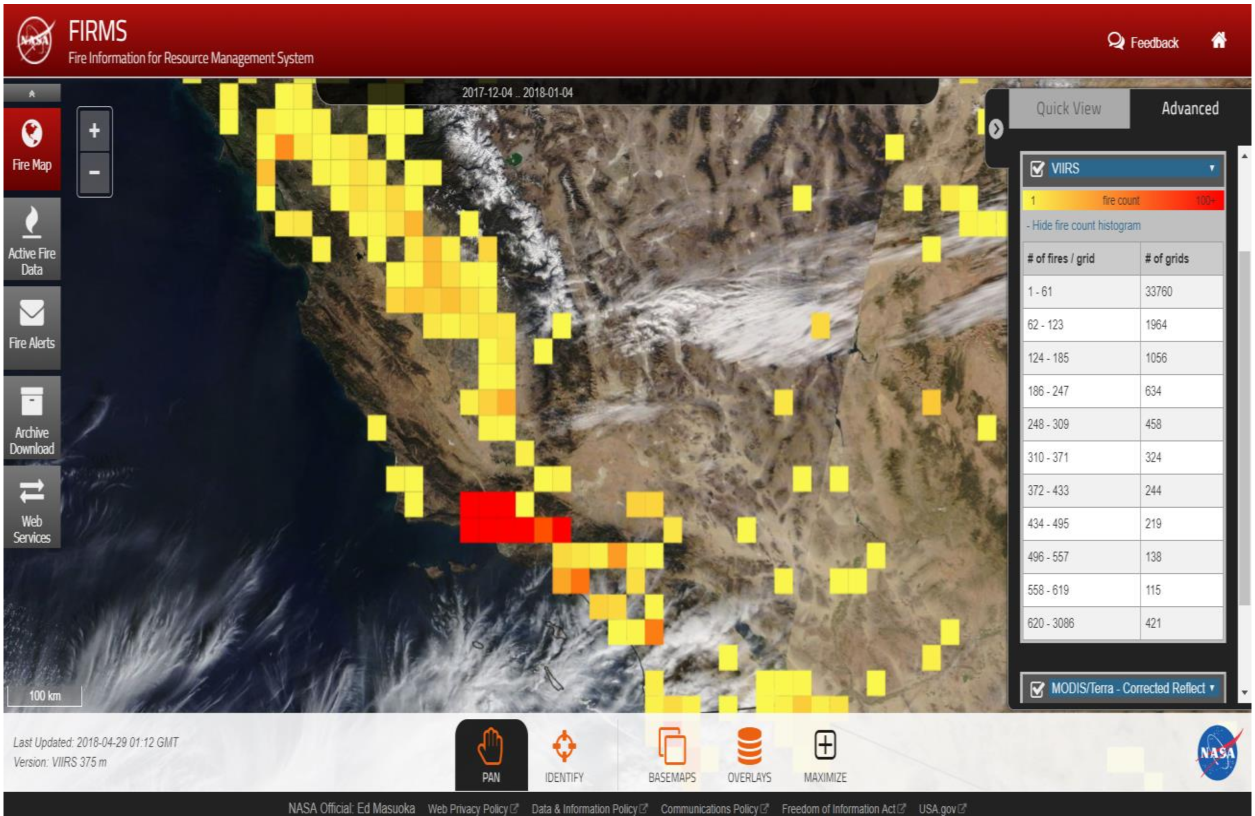

Modis fire product grid view collection

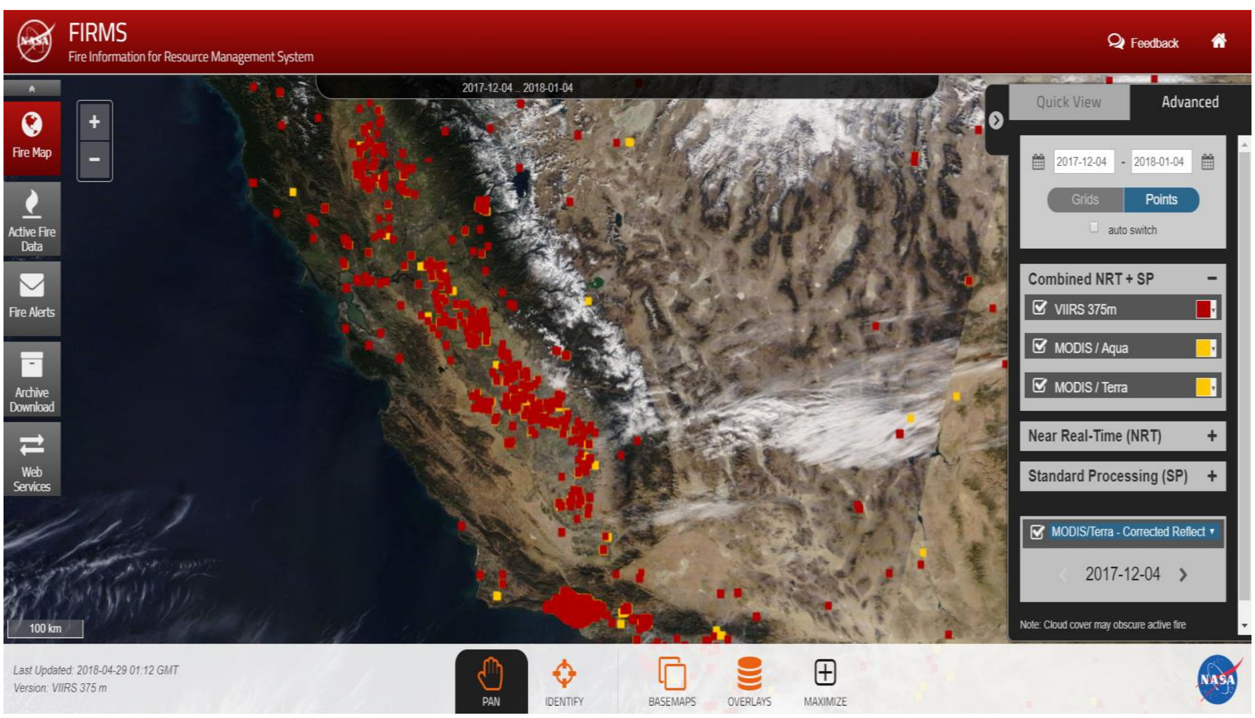

MODIS Fire product point collection

The obtained fire pixel raster was verified manually with the fire point shapefile by comparing them in ArcGIS Pro which gave an estimation of the number of pixels that were correctly classified as fire pixels and those which are not.

10. Conclusions & Possible Future Findings:

- Active fire spots are identified using fire detection algorithm.
- Accuracy Assessment was performed manually using MODIS fire points from FIRMS with an approximate accuracy of 70 – 80%
- Burn Severity Map is generated showing the Pre-Burn and Post Burn Scenario.
- Steady raise in Landsat class data may create new opportunities in the field of forest fire management activities
- With Landsat 9 possible launch in 2020, better quality of imagery can be obtained and analyzed using image processing techniques.
- With few more satellites launched the increase in temporal resolution can provide us with a better solution in detecting forest fires.

11. Literature Reviewed and References:

Wilfrid Schroeder, Patricia Oliva, Active fire detection using Landsat-8/OLI data. *Remote Sensing of Environment* 185 (2016) 210–220

Bastarrika. A.; Chuvieco, E. Martín, M.P. Mapping burned areas from Landsat TM/ETM+ data with a two phase algorithm: Balancing omission and commission errors. *Remote Sensing of Environment*. 2011. 105:1003-1012

R. McKinely, J. Clark, and J. Lecker, "Burn severity mapping in australia 2009," in International Archives of the Photogrammetry, Remote Sensing and Spatial Information Sciences, Melborne, Australia, August 25 – 01 September 2012, *ISPRS*, vol. XXXIX-B8, pp. 51–54.

Irons, J. R., Dwyer, J. L., & Barsi, J. A. (2012). the next landsat satellite: the landsat data continuity mission. *Remote Sensing of Environment*, 112, 11–21.

http://gsp.humboldt.edu/olm_2015/Courses/GSP_216_Online/lesson5-1/NBR.html

http://www.harrisgeospatial.com/Learn/Blogs/Blog-Details/TabId/2716/ArtMID/10198/ArticleID/15691/The-Many-Band-Combinations-of-Landsat-8.aspx

https://landsat.usgs.gov/using-usgs-landsat-8-product

https://earthdata.nasa.gov/earth-observation-data/near-real-time/firms/active-fire-data

https://landsat.gsfc.nasa.gov/landsat-data-continuity-mission/

https://firms.modaps.eosdis.nasa.gov

https://earthobservatory.nasa.gov/Features/Fire/